sparse inflorescence1 encodes a monocot-specific *YUCCA*-like gene required for vegetative and reproductive development in maize

Andrea Gallavotti*[†‡], Solmaz Barazesh[‡§], Simon Malcomber[¶], Darren Hall*, David Jackson[†], Robert J. Schmidt*, and Paula McSteen[§‖]

*Section of Cell and Developmental Biology, University of California at San Diego, La Jolla, CA 92093; [†]Cold Spring Harbor Laboratory, Cold Spring Harbor, NY 11724; [§]Department of Biology, Pennsylvania State University, University Park, PA 16802; and [¶]Department of Biological Sciences, California State University, Long Beach, CA 90840

Edited by Mark Estelle, Indiana University, Bloomington, IN, and approved August 1, 2008 (received for review June 10, 2008)

The plant growth hormone auxin plays a critical role in the initiation of lateral organs and meristems. Here, we identify and characterize a mutant, *sparse inflorescence1* (*spi1*), which has defects in the initiation of axillary meristems and lateral organs during vegetative and inflorescence development in maize. Positional cloning shows that *spi1* encodes a flavin monooxygenase similar to the *YUCCA* (*YUC*) genes of *Arabidopsis*, which are involved in local auxin biosynthesis in various plant tissues. In *Arabidopsis*, loss of function of single members of the *YUC* family has no obvious effect, but in maize the mutation of a single *yuc* locus causes severe developmental defects. Phylogenetic analysis of the different members of the *YUC* family in moss, monocot, and eudicot species shows that there have been independent expansions of the family in monocots and eudicots. *spi1* belongs to a monocot-specific clade, within which the role of individual *YUC* genes has diversified. These observations, together with expression and functional data, suggest that *spi1* has evolved a dominant role in auxin biosynthesis that is essential for normal maize inflorescence development. Analysis of the interaction between *spi1* and genes regulating auxin transport indicate that auxin transport and biosynthesis function synergistically to regulate the formation of axillary meristems and lateral organs in maize.

auxin biosynthesis | auxin transport | yucca | meristem

The plant hormone auxin is required for initiation and polar growth of all organ primordia. Auxin is synthesized by a number of pathways in the cell and is transported from cell to cell by diffusion and by the activity of influx and efflux carriers (1). During vegetative development, auxin is required for many developmental processes, including leaf and lateral root initiation, whereas during inflorescence development, auxin is required for the initiation of floral meristems (FMs) and floral organs (2–5). Extensive research in *Arabidopsis* has shown the importance of auxin transport during lateral organ and axillary meristem initiation (3–5). In addition, recent work has highlighted the role of localized auxin biosynthesis in all aspects of plant development (6–10). The role of auxin in monocots such as maize is not as well understood. Although some aspects of the control of auxin transport seem to be conserved between monocots and eudicots (11–16), there are also key differences (17).

Maize plants produce separate male and female inflorescences (18). The male inflorescence, the tassel, is situated at the shoot apex, whereas the female inflorescence, the ear, is produced from an axillary meristem several nodes below the tassel. The tassel consists of a main spike with several long lateral branches at the base (Fig. 1 *A* and *B*). Both the main spike and branches are covered with short branches, each of which bears a pair of spikelets. Each spikelet produces two leaf-like glumes that enclose a pair of florets. Florets consist of a lemma and palea (outer whorl structures derived from bracts or sepals), two lodicules (derived from petals), and three stamens in the tassel or a central carpel in the ear. Early development of both tassel and ear is similar, and selective abortion of organs later in development causes the production of unisexual inflorescences (19).

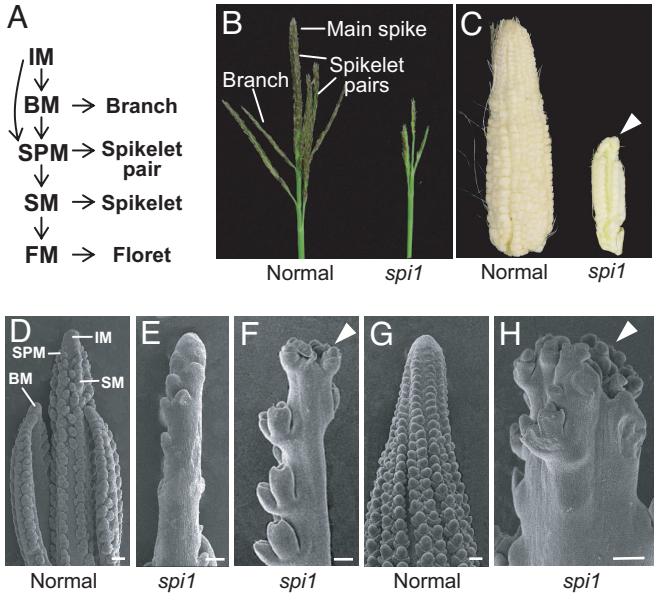

Fig. 1. Characterization of the *spi1* inflorescence. (*A*) Schematic of the different types of axillary meristem initiated during maize inflorescence development (*Left*) and the structures they produce (*Right*). (*B*) Tassels of normal (*Left*) and *spi1* (*Right*), showing reduced numbers of branches and spikelets in the *spi1* mutant. (*C*) Ears of normal and *spi1*, showing reduced kernel number as well as production of kernels over the tip (arrowhead) of *spi1* ears. (*D–H*) Scanning electron microscope images of developing *spi1* tassels and ears. (*D*) Normal tassel. (*E*) *spi1* tassel showing fewer SPMs. (*F*) Close-up of tip of *spi1* tassel later in development showing defective apical inflorescence meristem with SMs initiating over the tip (arrowhead). (*G*) Normal ear. (*H*) *spi1* ear showing fewer SPMs. The tip is fasciated and produces SMs (arrowhead). (Scale bars: 100 μm.)

Four types of axillary meristem produce the branched male inflorescence (20). The first is the branch meristem (BM), which

Author contributions: A.G., S.B., S.M., D.J., R.J.S., and P.M. designed research; A.G., S.B., S.M., and D.H. performed research; D.J. contributed new reagents/analytic tools; A.G., S.B., S.M., R.J.S., and P.M. analyzed data; and A.G., S.B., S.M., D.J., R.J.S., and P.M. wrote the paper.

The authors declare no conflict of interest.

This article is a PNAS Direct Submission.

Data deposition: The sequences reported in this paper have been deposited in the GenBank database [EU910940–41 (maize *spi1*) and EU913464 (Joinvillea *spi1*)].

[‡]A.G. and S.B. contributed equally to this work.

[‖]To whom correspondence should be addressed. E-mail: pcm11@psu.edu.

This article contains supporting information online at www.pnas.org/cgi/content/full/0805596105/DCSupplemental.

Table 1. Quantification of *spi1* and *bif2* single and double mutant phenotypes

Genotype	Branch number*	Spikelet number*	Plant height, cm†	Leaf number†
Normal	9.5 ± 0.7	585 ± 10.5	177.2 ± 3.8	19.2 ± 0.2
spi1	4 ± 0.6‡	66.3 ± 6.5‡	160.8 ± 5.7‡	17.9 ± 0.4‡
bif2	0.4 ± 0.2‡	25 ± 3.9‡	154 ± 7.8‡	17.2 ± 0.6‡
spi1;bif2	0 ± 0§	0.12 ± 0.3§	92 ± 12.4§	13.4 ± 1§

*n = 10 for each genotype.
†n = 120 for the segregating family.
‡Value is significantly different from normal, $P < 0.05$.
§Value is significantly different from either single mutant, $P < 0.05$.

is indeterminate and produces the long branches at the base of the tassel (Fig. 1*A*). Several long branches are produced before the determinate spikelet pair meristems (SPMs) are formed. SPMs produce short branches bearing the spikelet pairs. Spikelets are produced from spikelet meristems (SMs), which then transition to FMs, which give rise to florets and floral organs. The female inflorescence develops similarly except that it does not produce BMs.

Genes required for the initiation of axillary meristems in maize have been identified by characterization of two mutants with a barren phenotype: *barren stalk1* (*ba1*) and *barren inflorescence2* (*bif2*) (12, 21–23). *bif2* encodes a serine/threonine protein kinase co-orthologous to *PINOID* (*PID*), which functions in the regulation of polar auxin transport in *Arabidopsis* (12, 24–28). *bif2* mutants have a reduced number of branches, spikelets, florets, and floral organs in both tassel and ear (21). Double mutants between *bif2* and *teosinte branched1* (*tb1*), a mutation that causes the outgrowth of vegetative axillary meristems, show that *bif2* also plays a role in initiation of axillary meristems during vegetative development (12, 29). In addition, *bif2* has vegetative phenotypes, such as a reduction in plant stature and leaf number (12). These phenotypes and the *bif2* expression pattern indicate that *bif2* plays a role in both lateral organ and axillary meristem initiation. BIF2 interacts with and phosphorylates BA1, a basic helix–loop–helix transcription factor required for axillary meristem initiation (17, 23).

To further understand the mechanisms regulating axillary meristem initiation, we isolated and characterized a novel barren mutant, *sparse inflorescence1* (*spi1*), with defects in the formation of branches, spikelets, florets, and floral organs. *spi1* encodes a flavin monooxygenase with similarity to the *YUCCA (YUC)* genes of *Arabidopsis*, which catalyze the rate-limiting step in one of the tryptophan-dependent auxin biosynthetic pathways (6). Unlike *Arabidopsis*, in which knockouts of at least two *YUC* genes are required to see developmental defects (7, 8), single *spi1* loss of function mutants have a dramatic phenotype, with a significant reduction in the number of axillary meristems and lateral organs. Phylogenetic analyses suggest that this could be explained by a specific inflorescence development function acquired by *spi1*, together with the independent expansion of the *YUC* family in monocots and eudicots. In addition, double mutants between *spi1* and *bif2* have a synergistic interaction that demonstrates the role of *spi1* and *bif2* in vegetative development. These findings emphasize the importance of both auxin biosynthesis and auxin transport during lateral organ and axillary meristem initiation in maize.

Results and Discussion

***spi1* Mutants Have Defects During Vegetative and Reproductive Development.** *spi1* tassels have fewer branches and spikelets, and *spi1* ears are small, with fewer kernels (Fig. 1 *B* and *C*). Quantitative analysis of the mature tassel phenotype showed that *spi1* mutants have a reduction in branch and spikelet number, suggesting a defect in BM and SPM initiation (Table 1). We used scanning electron microscopy of immature tassel and ear to determine whether the reduction in BMs and SPMs in *spi1* inflorescences were the result of a failure to initiate these meristems or a failure to maintain their growth. In wild-type maize plants, BMs and SPMs were visible on the flanks of the inflorescence (Fig. 1*D*). In contrast, the surface of the *spi1* mutant tassel was smooth, with very few SPMs (Fig. 1*E*). Similarly, in the ear, a reduction in the number of SPMs was clearly visible (Fig. 1*H*). This analysis shows that the reduction in branch and spikelet number is caused by the failure to produce both BMs and SPMs.

Analysis of the mature tassel phenotype also revealed that *spi1* tassels were reduced to approximately three quarters of the length of normal tassels (Fig. 1*B*, data not shown), and mature ears displayed a similar reduction in size (Fig. 1*C*). To investigate the cause of the defect in the inflorescence meristem, we performed scanning electron microscopy analysis on later stages of tassel development. Analysis of *spi1* mutants showed that, unlike normal, SPMs grew over the tip of the inflorescence (arrowhead, Fig. 1*F*). The growth of spikelets over the inflorescence tip was also observed in the ear (arrowheads, Fig. 1 *C* and *H*), showing that *spi1* inflorescences have additional defects in the apical inflorescence late in development.

Spikelet and FM initiation was also defective in *spi1* mutants. Only approximately half of *spi1* spikelets produced the normal two florets per spikelet, whereas the remaining spikelets contained one or no florets (Table 2). The number of floral organs was also reduced, with most *spi1* florets producing less than the full complement of stamens (Table 2). This indicates that SMs and FMs are also defective, and thus all four types of reproductive axillary meristems are affected in *spi1* mutants.

To determine whether *spi1* also functioned in axillary meristem initiation during vegetative development, we constructed double mutants between *spi1* and *tb1*. The *tb1* mutant has a highly branched phenotype because all normally quiescent vegetative axillary meristems elongate to produce branches called tillers (29). *spi1;tb1* double mutants produced fewer tillers compared with *tb1* single mutants [supporting information (SI) Fig. S1], indicating that *spi1* also plays a role in axillary meristem initiation during vegetative development.

***spi1* Encodes a *YUCCA*-like Flavin Monooxygenase.** The *spi1–01-008–16* mutant, generated by EMS mutagenesis, was initially mapped to chromosome 3 by linkage to the SSR marker *umc2008*. By screening a mapping population of 210 mutant individuals, *spi1* was mapped to between markers AZM5_96828 (2 recombinants (R)/420 chromosomes) and *umc1320* (7R/420). A syntenic region in both rice and sorghum was identified, and

Table 2. Quantification of floret and floral organ number in *spi1* mutant spikelets

Genotype	% spikelets with			% florets with			% florets with			
	2 florets	1 floret	0 florets	2 lemma/palea	1 lemma/palea	0 lemma/palea	3 stamens	2 stamens	1 stamen	0 stamens
Normal	100	0	0	98	2	0	98	2	0	0
spi1	52	20	28	87	10	3	14	39	36	12

n = 100 each.

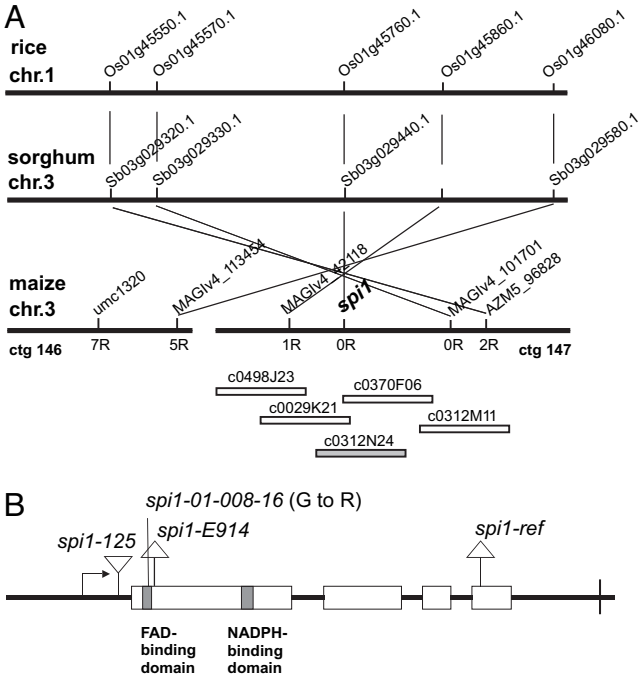

Fig. 2. Cloning of *spi1*. (*A*) Schematic representation of the positional cloning of the *spi1* gene. Black bars represent chromosomal segments of rice, sorghum, and maize (not to scale). Predicted genes for both rice and sorghum are indicated. In maize, the region encompasses two BAC contigs (FPC contigs 146 and 147). The number of recombinants (R) is shown below each maize marker. Empty rectangles represent BAC clones, and the filled rectangle indicates the BAC clone containing *spi1*. (*B*) *spi1* gene structure. Exons are represented as rectangles, mRNA sequence is indicated between the arrow and the vertical bar. The putative enzymatic sites of the YUC proteins are shown in gray. Upward and downward triangles symbolize deletions and insertion, respectively, in the corresponding *spi1* mutant alleles.

markers were developed for the corresponding maize genes (Fig. 2*A*). These markers were used to delimit the *spi1* locus to a region on FPC contig 147 between markers MAGIv4_42118 (1R/420) and AZM5_96828. Analysis of the region in rice and sorghum identified several candidate genes, including a predicted flavin monooxygenase with similarity to the *Arabidopsis YUC* genes (6), which was found to be closely linked to the *spi1* locus (0R/420). The sequence of the corresponding maize *YUC* gene was obtained by database search and RT-PCR. This gene was sequenced in the *spi1–01-008–16* allele, and a point mutation was identified in the highly conserved flavin adenine dinucleotide binding domain, causing a glycine-to-arginine change that was not present in the progenitor (Fig. 2*B*). Sequencing of three additional *spi1* alleles identified two in-frame deletions in conserved regions of *spi1* (*spi1-E914* and *spi1-ref*) and an insertion of a *Mutator* transposable element in the 5′ untranslated region (*spi1–125*) (Fig. 2*B* and Fig. S2). These lesions in four independent *spi1* alleles show unequivocally that the *spi1* gene encodes a *YUC*-like flavin monooxygenase.

***spi1* Expression Is Localized in Proximity to Newly Emerging Primordia and Axillary Meristems.** *spi1* expression was detected by RT-PCR in all tissues tested except root and endosperm (Fig. 3*A*). To investigate the localization of *spi1* expression during inflorescence development, RNA *in situ* hybridization was performed on immature tassel and ear. Early in development, *spi1* expression was first observed on the flanks of the inflorescence, presumably marking the newly forming SPMs (arrowhead, Fig. 3*B*). Subsequently, this expression was retained on the adaxial side of emerging SPMs (Fig. 3*C*). *spi1* was also expressed in SPMs in the

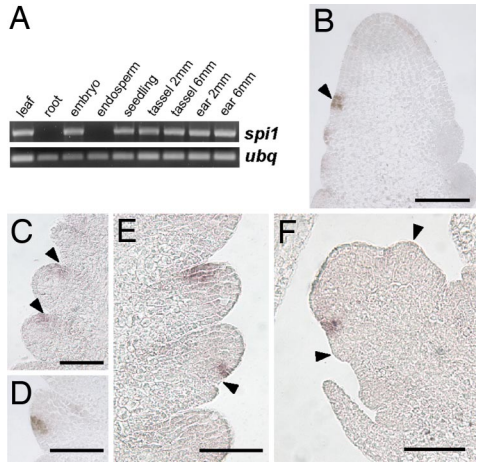

Fig. 3. *spi1* expression analysis. (*A*) *spi1* qualitative RT-PCR in different tissue samples. *ubq, ubiquitin* as control. (*B–F*) *spi1* RNA *in situ* hybridization in young inflorescences. (*B*) *spi1* expression marks the site of new SPM formation (arrowhead). (*C* and *D*) Developing SPMs. (*E*) An SM giving rise to the lower FM (arrowhead). (*F*) Floral meristem forming stamen primordia (arrowheads). (Scale bars: 20 μm.)

process of forming SMs (Fig. 3*D*). In SMs, *spi1* became localized to just a few cells adaxial to where the lower FM will develop (Fig. 3*E*). As floral organs initiated, *spi1* was expressed in a small group of cells proximal to the developing floral organs (Fig. 3*F*). The domain of *spi1* expression was consistently limited to the two outermost meristem layers. In summary, *spi1* was transiently expressed in a few cells proximal to newly emerging axillary meristems and lateral primordia at each stage of inflorescence development. Expression analysis of *Arabidopsis* and *Petunia YUC*-like genes also revealed distinct temporal and spatial expression patterns during inflorescence and flower development (7, 8, 30). These observations suggest that localized auxin biosynthesis is required for normal axillary meristem and lateral organ initiation during maize inflorescence development.

Phylogenetic Analysis Shows That *spi1* Is a Member of a Monocot-Specific Clade of *YUC*-Like Genes. Bayesian phylogenetic analyses of 62 land plant *YUC*-like genes, rooted using two fungal sequences, estimates a well-supported (>95% clade credibility [CC]) monocot clade comprising the grass species *Zea mays spi1*, *Oryza sativa YUC1* (*OsYUC1*; Os1g064540/Os1g45760), *Sorghum bicolor* Sb03g029440, and *Joinvillea ascendens JaSPI1*, an immediate relative of grasses (Fig. 4). The *spi1* clade is sister to a well-supported clade containing two lineages of grass *YUC*-like genes including *OsYUC4* and *OsYUC5* (31). The phylogeny estimates that the *spi1*, *OsYUC4*, and *OsYUC5* clades are products of duplications within monocots and have no clear co-orthologue in eudicots. The *spi1*/*OsYUC4*/*OsYUC5* clade is sister to a clade containing both monocot and eudicot sequences, including *Arabidopsis AtYUC1*, *-2*, *-4*, and *-6* and the rice genes *OsYUC2* and *OsYUC3* (6, 7, 31). Within this clade, *AtYUC1* and *YUC4* are nested within a well-supported eudicot clade, with *AtYUC4* co-orthologous to *Petunia* and tomato *FLOOZY* (*PhFZY* and *ToFZY*, respectively) (30, 32). An additional well-supported eudicot clade containing *AtYUC3*, *-5*, *-7*, *-8*, and *-9* suggests that *AtYUC3* and *-7*, as well as *AtYUC5*, *-8*, and *-9*, are products of gene duplications since poplar and *Arabidopsis* last shared a common ancestor. The clade containing the previously characterized rice *OsYUC8*/*NARROW LEAF7 (NAL7)*/*OsCONSTITUTIVELY WILTED (OsCOW1)* (33, 34) gene is sister to the clade containing *AtYUC1* to *-9* and *OsYUC1* to *-7* and is estimated to have diverged from these other eudicot and monocot genes near

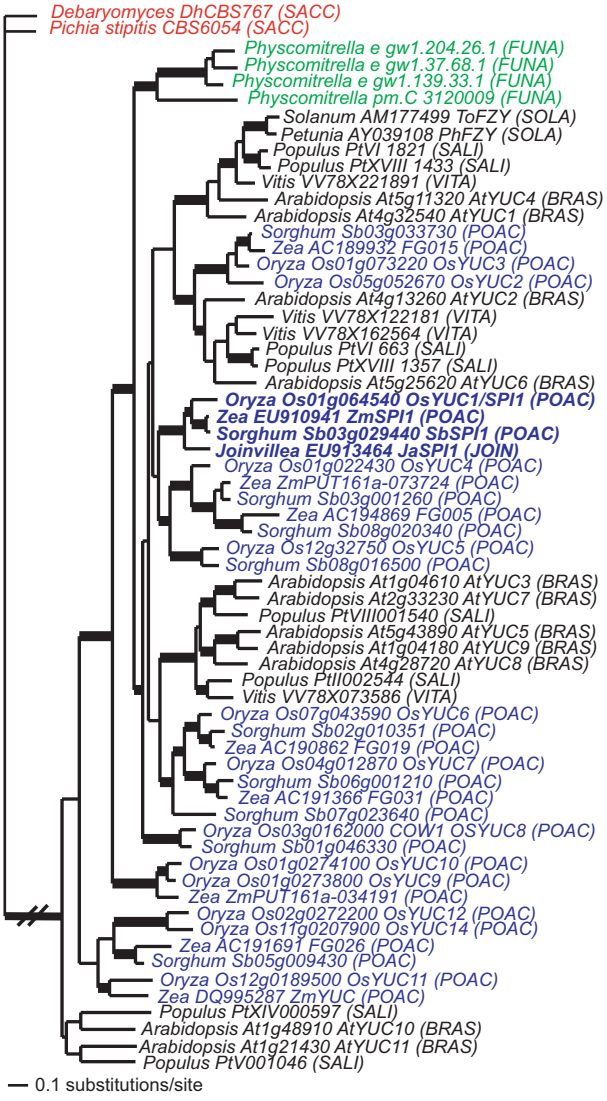

Fig. 4. Phylogenetic analysis of *YUC*-like genes from diverse land plants. Bayesian consensus phylogram of 62 *YUC*-like genes from land plants rooted using two fungal sequences (*Debaryomyces DhCBS767* and *Pichia PsCBS6054*). Thick branches supported by >0.95 CC. Fungi (red): SACC = *Saccharomycetaceae*; Moss (green): FUNA = *Funariaceae*; Angiosperm-eudicot (black): BRAS = *Brassicaceae*, SALI = Salicaceae, SOLA = *Solanaceae*, VITA = *Vitaceae*; Angiosperm-monocot (blue): JOIN = *Joinvilleaceae*, POAC = *Poaceae*. Maize *spi1* and orthologues in rice (*OsYUC1*), sorghum (Sb03g029440), and *Joinvillea* (*JaSPI1*) in bold.

the base of the flowering plant clade. On the basis of the position of the moss (*Physcomitrella patens*) sequences, the clade containing *AtYUC1* to *-9* and *OsYUC1* to *-8* originated within land plants, so *spi1* last shared a common ancestor with the *AtYUC* genes 125–450 MYA. *AtYUC10* and *-11* and *OsYUC9* to *-14* are more distantly related to the other eudicot and monocot *YUC* genes, having diverged before the origin of land plants.

Therefore, phylogenetic analysis reveals an ancient origin of *YUC*-like genes in land plants, with several lineage-specific gene duplication events in monocots and eudicots leading to a complex pattern of relationships. Maize *spi1* is orthologous to rice *OsYUC1* and sorghum Sb03g029440 (on the basis of both synteny and sequence) and *Joinvillea JaSPI1* (on the basis of sequence) and is estimated to have originated from a gene duplication event within the monocot clade. However, expression and functional analyses reveal that the roles of *OsYUC1* and *spi1* in plant development have diverged. *OsYUC1* expression is detected in all tissues, including roots, by RT-PCR analysis (31). Within the inflorescence, *OsYUC1* is localized in the vasculature rather than axillary meristems using a GUS reporter assay (31). In contrast, *spi1* is expressed in most tissues except roots and endosperm, and within the inflorescence *spi1* is expressed in axillary meristems and not in the vasculature. Furthermore, *OsYUC1* knockdown mutants are dwarfed owing to severe defects in both shoot and root elongation, but no inflorescence phenotype was reported (31). *spi1* mutant plants are slightly shorter than normal plants, but the most distinctive phenotype is the defective initiation of axillary meristems in the inflorescences. These data indicate that there has been a change of *OsYUC1*/*spi1* expression and function during the diversification of the grass family.

The relationship of the grass *spi1* clade to eudicots is complex owing to the multiple rounds of genome duplication in monocots and eudicots. Although not strongly supported in our phylogenetic analysis (90% CC), the Bayesian consensus phylogram estimates a sister relationship between the *spi1*/*OsYUC1*, *OsYUC4*, and *OsYUC5* clade and a clade containing both eudicot *AtYUC1*, *-2*, *-4*, and *-6* and monocot members *OsYUC2* and *-3*. In support of this relationship, *Arabidopsis yuc1;yuc2;yuc4;yuc6* quadruple mutants and *Petunia fzy* mutants have some phenotypes in common with maize *spi1* mutants (7, 30). Additional *Petunia* sequences are not available, but the mutant phenotype suggests that *FZY* plays an important role in *Petunia*. Furthermore, the phylogenetic and genetic analyses suggest that *spi1* might be the dominant gene regulating auxin biosynthesis in maize inflorescence development, with the maize orthologues of *OsYUC2* to *-5* hypothesized to have largely redundant and reduced roles during inflorescence development.

Interaction of *spi1* with Genes Regulating Auxin Transport. *bif2* mutants have a similar phenotype to *spi1* mutants, with a reduced number of tassel branches and spikelets due to defects in axillary meristem initiation (Fig. 5*A*) (21). Because *bif2* encodes a *PID*-like serine/threonine kinase proposed to play a role in auxin transport (12, 24–28), and *spi1* encodes an enzyme that functions in auxin biosynthesis (6, 7), we constructed *spi1;bif2* double mutants to investigate the interaction between these two pathways. *spi1;bif2* double mutants displayed a synergistic phenotype, with severe defects in both vegetative and reproductive development (Fig. 5 *A* and *B*). *spi1;bif2* mutants produced a completely barren tassel, with no branches or spikelets (Fig. 5*A* and Table 1). Whole plant architecture was dramatically affected (Fig. 5*B*). Although *spi1* and *bif2* single mutants had a slight reduction in plant height, *spi1;bif2* double mutants were reduced to approximately half the height of normal plants (Table 1). To determine whether the reduction in height was due to a reduction in the number of phytomers produced, we counted the number of leaves. *spi1* and *bif2* single mutants produced one or two fewer leaves than normal, but *spi1;bif2* mutants produced on average six leaves fewer than their normal sibs (Table 1). Therefore, *spi1* and *bif2* (together with other factors) regulate leaf production during vegetative development.

To further investigate the interaction between auxin biosynthesis and auxin transport, we crossed the *spi1* mutant with a *ZmPIN1a-YFP* maize reporter line (14). The *Arabidopsis* PIN family encodes auxin efflux carriers, and subcellular polar localization of PIN is an indication of the direction of auxin flow (35–37). In normal plants, confocal images of developing tassels showed that *ZmPIN1a-YFP* expression was upregulated at the site of axillary meristem initiation (Fig. 5*C*) (14). In *spi1* mutants, *ZmPIN1a-YFP* expression was absent where axillary meristems failed to initiate (Fig. 5*D*). Therefore, these results confirm that *spi1*-mediated auxin biosynthesis is required for upregulation of

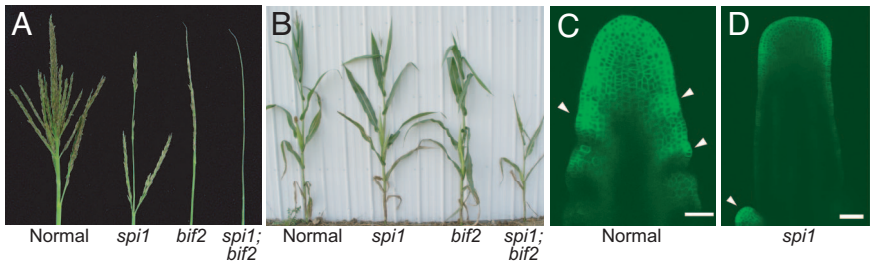

Fig. 5. Interaction between *spi1* and genes required for auxin transport. (*A*) Mature tassel phenotype showing all phenotypic classes in *spi1;bif2* family. (*B*) Whole plant phenotype of all phenotypic classes of *spi1;bif2* family. (*C* and *D*) *ZmPIN1a-YFP* expression in young tassels. (*C*) In normal plants, *ZmPIN1a-YFP* expression marks the emerging axillary meristems (arrowheads). (*D*) In *spi1* mutants, *ZmPIN1a-YFP* expression is absent on the flanks of the inflorescence when axillary meristems do not form. Expression is detected when axillary meristems have initiated (arrowhead). (Scale bars: 50 μm.)

ZmPIN1a expression during axillary meristem initiation in maize inflorescence development.

These results show there is an important interconnection between auxin biosynthesis and auxin transport, with both being required for plant development. Synergism between auxin biosynthesis and auxin transport has also been reported in *Arabidopsis* (8, 38). Because auxin plays a role in regulating its own efflux, and expression of *PIN* is auxin induced, an intimate feedback between auxin biosynthesis and transport is not unexpected (39, 40). Our results show that localized endogenous auxin biosynthesis is required for the proper upregulation of PIN1 to initiate a new axillary meristem. This provides a mechanistic understanding for the synergistic interaction between auxin biosynthesis and transport by proposing that localized auxin biosynthesis plays a role in inducing or regulating auxin transport components.

Conclusions

The *spi1* gene functions in the formation of axillary meristems and lateral organs throughout maize vegetative and reproductive development. *spi1* encodes a *YUC*-like gene related to genes described in eudicots but is a member of a monocot-specific clade. Expression and functional analysis indicates that diverse *YUC*-like genes play a role in the initiation of axillary meristems and lateral organs in distantly related flowering plants, including maize, *Petunia*, and *Arabidopsis* (7, 8, 30).

There are also important differences in *YUC* function between monocots and eudicots. For example, *yuc* double, triple, and quadruple mutants in *Arabidopsis* and *fzy* mutants in *Petunia* have a bushy phenotype due to reduced apical dominance (7, 30). However, *spi1* mutants have the opposite effect, with fewer branches due to the role of *spi1* in vegetative axillary meristems. Another unique aspect of the *spi1* phenotype is the production of spikelets over the tip of the apex, which implies that auxin biosynthesis plays a role in normal apical meristem function. Other *YUC*-like genes play diverse roles in leaf, root, and embryogenic development (8, 33, 34). Therefore, functional and phylogenetic analyses suggest that the *YUC* gene family has expanded in both eudicots and monocots with extensive functional diversification in different species. Furthermore, *spi1* and its ortholog in rice, *OsYUC1*, have differences in mutant phenotype and expression pattern (31), indicating a significant diversification of function even within the grass family. Our results show that *spi1* has evolved a very specific and localized role in auxin biosynthesis during maize inflorescence and vegetative development and suggest that even though the general mechanisms of auxin biosynthesis and transport seem to be widely conserved, the *YUC* gene family is capable of rapid functional divergence with the potential to generate novel plant morphologies.

Materials and Methods

***spi1* Alleles.** The *spi1-ref* allele was identified in a *Mutator* transposon mutagenesis screen. *spi1-125* and *spi1-E914* were obtained from the *RescueMu* population (http://www.maizegdb.org/rescuemu-phenotype.php). *spi1–01-008–16* was originally identified as a double mutant with a weak allele of *ramosa1* (*ra1-RS*) in an EMS enhancer/suppressor screen (A.G. and R.S., unpublished data). All phenotypic analysis was performed with the *spi1-ref* backcrossed into the B73 background eight times.

Scanning Electron Microscopy and Histology. Tassels were dissected from plants grown in the greenhouse to 5–7 weeks old, and ears were dissected from plants grown in the field to 8 weeks old. Fixation, scanning electron microscopy, and histology were performed as previously described (41).

***spi1* Cloning.** For positional cloning, an F2 mapping population was generated by crossing the *spi1;ra1-RS* double mutant with the maize inbred line B73. The *spi1* region was delimited by screening 210 F2 homozygous mutants using SSR markers. Syntenic regions in rice and sorghum were identified using rice (www.gramene.org) and sorghum (www.phytozome.net) sequences. New maize markers were designed (Table S1) using genome sequence information available at TIGR (http://maize.tigr.org) and at MAGI (http://magi.plantgenomics.iastate.edu). PCR primers SPI1-F1/SPI1-R1 and SPI1-F2/SPI1-R2 (Table S2) were used to amplify and sequence the *YUC*-like gene in the *spi1* alleles. Sequencing of multiple inbred lines verified that the in-frame deletion mutations (*spi1-ref* and *spi1-E914*) were not inbred polymorphisms.

Expression Analysis. For RT-PCR, five individual samples were pooled for each tissue tested (embryo 20 DAP, endosperm 20 DAP, root, seedling, immature leaves, immature tassels, and ears). Total RNA was extracted using TRIzol (Invitrogen) and further purified using the RNeasy Plant Mini kit (Qiagen). 1 μg of RNA was treated with DNase (Promega), and 12 ng of RNA was used in one-step RT-PCR reactions (One-step RT-PCR kit; Invitrogen). *spi1* was amplified with primers SPI1-F3/SPI1-R2 for 40 cycles, and the ubiquitin control was amplified for 30 cycles (Table S2). For RNA *in situ* hybridizations, a probe was constructed containing part of the coding sequence at the 3′ end of the gene and the 3′ UTR, amplified with SPI1-F2/SPI1-R2 (Table S2). Tissue samples were fixed in FAA (50% ethanol, 10% formaldehyde, and 5% acetic acid) for 2 h. Tissue preparation and *in situ* hybridization was performed as previously described (23).

***spi1* Phylogeny.** Sixty-three *YUC*-like genes were identified from moss (*Physcomitrella*), eudicots (*Arabidopsis*, grape, poplar, and tomato), and monocots (maize, rice, and sorghum) using BLAST searches at NCBI (http://www.ncbi.nlm.nih.gov/), PlantGDB (http://www.plantgdb.org), and CoGe (http://synteny.cnr.berkeley.edu/CoGe/). *Joinvillea SPI1* was isolated from young inflorescence cDNA using 3′ RACE RT-PCR with YUC-559F and polyT+ adaptor primers (Table S2). Two fungal sequences (*Debaryomyces* and *Pichia*) were used as outgroups. Nucleotide sequences were aligned on the basis of the conceptual amino acid translation using MacClade 4.0 (42) and ClustalX (43), before being adjusted manually using MacClade. Bayesian phylogenetic analyses used MrBayes 3.1 (44) on the Beowulf parallel processing cluster at the University of Missouri–St. Louis and comprised two separate searches of 5 million generations using default flat priors and the General Time Reversible model of evolution with gamma distributed rates and invariant sites (GTR+I+G). The aligned matrix was partitioned according to codon position and different parameters estimated for each partition. Trees were sampled every 200 generations, and burn-in trees were determined empirically by plotting the likelihood score against generation number and assessing parameter convergence. After burn-in trees had been removed, CC values and the 95% set of credible trees were estimated using MrBayes 3.1 (44).

***spi1* Double Mutant Analysis.** To construct double mutants between *spi1* and *bif2*, plants heterozygous for *spi1-ref* were crossed by plants heterozygous for

bif2–77 (12) in B73 and selfed. Segregation of phenotypic classes failed to be rejected by χ^2 tests (Table S3). Plants were genotyped for the *bif2–77* mutation as previously described (41) and for the *spi1-ref* deletion with primers SPI1-GF and SPI1-GR (Table S2). To construct double mutants between *spi1* and *tb1*, plants heterozygous for *spi1-ref* were crossed by *tb1-ref* in B73 (29). *spi1;tb1* double mutants were identified by tiller and tassel phenotype. Primary and secondary tiller number was counted at maturity.

Confocal Microscopy. The *spi1-01–008-16* mutant was crossed to the maize *ZmPIN1a-YFP* fluorescent marker line (14) and then selfed. Immature tassels (2–5 mm) were dissected and imaged as previously described (14).

ACKNOWLEDGMENTS. We thank L. Smith, G. Chuck, and S. Hake (Plant Gene Expression Center) for seed of the *spi1-ref* allele; the Maize Coop for seed of *spi1–125* and *spi1-E914*; A. Omeis and W. S. Harkcom for excellent plant care; D. Lorence (National Tropical Botanical Garden) for material of *Joinvillea ascendens*; Y. Zhao and members of the Jackson laboratory for helpful discussions; and the University of Missouri–St. Louis for access to the Beowulf computer cluster. This research was supported by United States Department of Agriculture/Cooperative State Research, Education, and Extension Service grant 2007–03036 (to P.M.); National Science Foundation grant DBI-0604923 in support of research by A.G., R.J.S., and D.J.; and National Science Foundation grant DBI-0501862 (to D.J.). A.G. was funded in part by a Cold Spring Harbor Laboratory Association Fellowship.

1. Delker C, Raschke A, Quint M (2008) Auxin dynamics: The dazzling complexity of a small molecule's message. *Planta* 227:929–941.
2. Benkova E, *et al.* (2003) Local, efflux-dependent auxin gradients as a common module for plant organ formation. *Cell* 115:591–602.
3. Okada K, *et al.* (1991) Requirement of the auxin polar transport system in early stages of *Arabidopsis* floral bud formation. *Plant Cell* 3:677–684.
4. Reinhardt D, *et al.* (2003) Regulation of phyllotaxis by polar auxin transport. *Nature* 426:255–260.
5. Reinhardt D, Mandel T, Kuhlemeier C (2000) Auxin regulates the initiation and radial position of plant lateral organs. *Plant Cell* 12:507–518.
6. Zhao YD, *et al.* (2001) A role for flavin monooxygenase-like enzymes in auxin biosynthesis. *Science* 291:306–309.
7. Cheng YF, Dai XH, Zhao YD (2006) Auxin biosynthesis by the YUCCA flavin monooxygenases controls the formation of floral organs and vascular tissues in *Arabidopsis*. *Gene Dev* 20:1790–1799.
8. Cheng Y, Dai X, Zhao Y (2007) Auxin synthesized by the YUCCA flavin monooxygenases is essential for embryogenesis and leaf formation in *Arabidopsis*. *Plant Cell* 19:2430–2439.
9. Tao Y, *et al.* (2008) Rapid synthesis of auxin via a new tryptophan-dependent pathway is required for shade avoidance in plants. *Cell* 133:164–176.
10. Stepanova AN, *et al.* (2008) TAA1-mediated auxin biosynthesis is essential for hormone crosstalk and plant development. *Cell* 133:177–191.
11. Scanlon MJ (2003) The polar auxin transport inhibitor N-1-naphthylphthalamic acid disrupts leaf initiation, KNOX protein regulation, and formation of leaf margins in maize. *Plant Physiol* 133:597–605.
12. McSteen P, *et al.* (2007) *barren inflorescence2* encodes a co-ortholog of the PINOID serine/threonine kinase and is required for organogenesis during inflorescence and vegetative development in maize. *Plant Physiol* 144:1000–1011.
13. Wu X, McSteen P (2007) The role of auxin transport during inflorescence development in maize, *Zea mays* (Poaceae). *Am J Bot* 11:1745–1755.
14. Gallavotti A, Yang Y, Schmidt RJ, Jackson D (2008) The relationship between auxin transport and maize branching. *Plant Physiol* 147:1913–1923.
15. Morita Y, Kyozuka J (2007) Characterization of. *OsPID*, the rice ortholog of *PINOID*, and its possible involvement in the control of polar auxin transport. *Plant Cell Physiol* 48:540–549.
16. Xu M, Zhu L, Shou HX, Wu P (2005) A PIN1 family gene, *OsPIN1*, involved in auxin-dependent adventitious root emergence and tillering in rice. *Plant Cell Physiol* 46:1674–1681.
17. Skirpan A, Wu X, McSteen P (2008) Genetic and physical interaction suggest that BARREN STALK 1 is a target of BARREN INFLORESCENCE2 in maize inflorescence development. *Plant J* 55:787–797.
18. McSteen P, Laudencia-Chingcuanco D, Colasanti J (2000) A floret by any other name: Control of meristem identity in maize. *Trends Plants Sci* 5:61–66.
19. Irish EE (1996) Regulation of sex determination in maize. *Bioessays* 18:363–369.
20. Irish EE (1997) Class II *tassel seed* mutations provide evidence for multiple types of inflorescence meristems in maize (*Poaceae*). *Am J Bot* 84:1502–1515.
21. McSteen P, Hake S (2001) *barren inflorescence2* regulates axillary meristem development in the maize inflorescence. *Development* 128:2881–2891.
22. Ritter MK, Padilla CM, Schmidt RJ (2002) The maize mutant *barren stalk1* is defective in axillary meristem development. *Am J Bot* 89:203–210.
23. Gallavotti A, *et al.* (2004) The role of *barren stalk1* in the architecture of maize. *Nature* 432:630–635.
24. Christensen SK, Dagenais N, Chory J, Weigel D (2000) Regulation of auxin response by the protein kinase PINOID. *Cell* 100:469–478.
25. Benjamins R, *et al.* (2001) The PINOID protein kinase regulates organ development in *Arabidopsis* by enhancing polar auxin transport. *Development* 128:4057–4067.
26. Friml J, *et al.* (2004) A PINOID-dependent binary switch in apical-basal PIN polar targeting directs auxin efflux. *Science* 306:862–865.
27. Lee SH, Cho HT (2006) PINOID positively regulates auxin efflux in *Arabidopsis* root hair cells and tobacco cells. *Plant Cell* 18:1604–1616.
28. Michniewicz M, *et al.* (2007) Antagonistic regulation of PIN phosphorylation by PP2A and PINOID directs auxin flux. *Cell* 130:1044–1056.
29. Doebley J, Stec A, Hubbard L (1997) The evolution of apical dominance in maize. *Nature* 386:485–488.
30. Tobena-Santamaria R, *et al.* (2002) FLOOZY of petunia is a flavin mono-oxygenase-like protein required for the specification of leaf and flower architecture. *Gene Dev* 16:753–763.
31. Yamamoto Y, *et al.* (2007) Auxin biosynthesis by the YUCCA genes in rice. *Plant Physiol* 143:1362–1371.
32. Esposito-Rodriguez M, *et al.* (2007) Cloning and biochemical characterization of *ToFZY*, a tomato gene encoding a flavin monooxygenase involved in a tryptophan-dependent auxin biosynthesis pathway. *J Plant Growth Regul* 26:329–340.
33. Fujino K, *et al.* (2007) *NARROW LEAF 7* controls leaf shape mediated by auxin in rice. *Mol Genet Genomics* 279:499–507.
34. Woo YM, *et al.* (2007) *CONSTITUTIVELY WILTED1*, a member of the rice YUCCA gene family, is required for maintaining water homeostasis and an appropriate root to shoot ratio. *Plant Mol Biol* 65:125–136.
35. Galweiler L, *et al.* (1998) Regulation of polar auxin transport by AtPIN1 in *Arabidopsis* vascular tissue. *Science* 282:2226–2230.
36. Petrasek J, *et al.* (2006) PIN proteins perform a rate-limiting function in cellular auxin efflux. *Science* 312:914–918.
37. Wisniewska J, *et al.* (2006) Polar PIN localization directs auxin flow in plants. *Science* 312:883.
38. Cheng Y, Qin G, Dai X, Zhao Y (2007) NPY1, a BTB-NPH3-like protein, plays a critical role in auxin-regulated organogenesis in *Arabidopsis*. *Proc Nat Acad Sci USA* 104:18825–18829.
39. Vieten A, *et al.* (2005) Functional redundancy of PIN proteins is accompanied by auxin dependent cross-regulation of PIN expression. *Development* 132:4521–4531.
40. Paciorek T, *et al.* (2005) Auxin inhibits endocytosis and promotes its own efflux from cells. *Nature* 435:1251–1256.
41. Barazesh S, McSteen P (2008) *barren inflorescence1* functions in organogenesis during vegetative and inflorescence development in maize. *Genetics* 179:389–401.
42. Maddison DR, Maddison WP (2003) *MacClade: Analysis of Phylogeny and Character Evolution* (Sinauer Associates, Sunderland, MA).
43. Jeanmougin F, *et al.* (1998) Multiple sequence alignment with Clustal X. *Trends Biochem Sci* 23:403–405.
44. Huelsenbeck JP, Ronquist F (2001) MRBAYES: Bayesian inference of phylogenetic trees. *Bioinformatics* 17:754–755.